Supplementary Materials

Censor-aware semi-supervised survival time prediction in lung cancer using clinical and radiomics features

Arman Groji¹, Ali Fathi Jouzdani¹, Nima Sanati¹, Ren Yuan^{2,3}, Arman Rahmim^{3,4}, Mohammad R. Salmanpour^{3,4,5}

Correspondence to: Mohammad R. Salmanpour, Department of Basic and Translational Research, BC Cancer Research Institute, Vancouver V5Z 1L3, Canada. E-mail: msalman@bccrc.ca

1. Methods and Material

Supplemental Table S1. Clinical features description

Features	Meaning
Surgary cotagony	The types of surgery that patients have such as
Surgery category	'pneumonectomy', 'lobectomy', 'segmentectomy
Ethnicity	Tells the patient is Asian or not.
Postoperative residual	Explains post-operation residual tumor with 'Microscopic',
tumor	'Macroscopic', and 'Not Applicable' values
Primary tumour	Describes Primary Tumour Resected in surgery with 'Yes',
resected	'No', and 'Not Applicable' values
Radiation therapy	Shows if a person has radiation therapy or not

¹Department of Neuroscience, Hamadan University of Medical Sciences, Hamadan 65176-19657, Iran.

²BC Cancer, Vancouver Center, Vancouver V5Z 4E6, Canada.

³Department of Radiology, University of British Columbia, Vancouver V5Z 1M9, Canada.

⁴Department of Basic and Translational Research, BC Cancer Research Institute, Vancouver V5Z 1L3, Canada.

⁵Technological Virtual Collaboration (TECVICO CORP.), Vancouver V5E 3H7, Canada.

arcinoma,
ding current
nount a person
calculated by
es smoked per
moked
e others don't.
same place it
he cancer has
e it first started.
e back in
n where it
r not
physically
o carry out
oulatory and
ut any work
are, 4—
date

1.1.Image preprocessing and mask preparation

1.1.1. Attenuation correction (AC)

Attenuation correction (AC) is one of the most important corrections that need to be performed in PET imaging. AC methods aim to account for the photon attenuation

along each line of response (LOR). For this purpose, maps of the linear attenuation coefficients (LACs) for all the tissues and materials located in the PET field of view are generated or integrals of these values along all the LORs are directly measured. The procedure for including this information in the reconstruction (performing the actual correction) is similar [1].

1.1.2. Standardized Uptake Value (SUV) correction

SUV is a quantitative measure used in PET imaging to supplement visual interpretation of PET images. It is a ratio of tissue radioactivity concentration to injected dose per unit body weight, normalized to the whole-body radioactivity concentration. SUV is a semiquantitative measure, simpler to calculate than fully quantitative measures like the influx constant K. It can be corrected for factors like body weight, lean body mass, and body surface area [2].

1.1.3. Min/max normalization technique

Min-max normalization is a technique that transforms the values of a numerical variable to a standard range, usually between 0 and 1. It is useful for comparing data that have different scales or units of measurement. The formula for min-max normalization is:

$$x' = (x - min) / (max - min)$$

where x is the original value, x' is the normalized value, min is the minimum value of the variable, and max is the maximum value of the variable. This technique is also known as feature scaling or rescaling [3, 4].

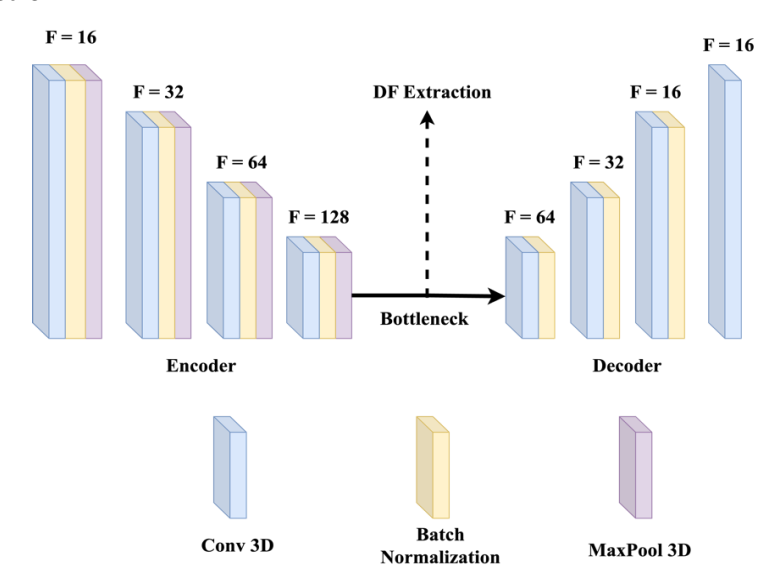
1.2. Feature extraction

1.2.1. HRF Extraction

In our investigation, we utilized two distinct strategies for image feature extraction: HRF and DRF. Within the HRF strategy, a total of 215 quantitative HRFs were derived from each delineated tumor region using the PySERA standardization process available in the ViSERA software [5]. The radiomic feature generation process in ViSERA aligns with the protocols established by the Image Biomarker Standardization Initiative (ISBI). The 215 HRFs encompassed a variety of feature types: 29 shape descriptors, 20 first-order statistics (FO), 30 intensity histogram parameters (IH), and 136 textural features. These textural features included 50 co-

occurrence matrix attributes (CMs), 32 run-length matrix characteristics (RLMs), 16 size zone metrics (SZMs), 16 distance zone parameters (DZMs), 5 neighborhood gray-tone difference matrix elements (NGTs), and 17 neighboring gray level dependence matrix indices (NGLs). HRFs were extracted from the segmented PET and CT images.

1.2.2. DRF Extraction



Supplemental Figure S1. Structure of our autoencoder model. The Encoder includes four convolutional layers, each followed by a batch normalization and a max-pooling operation. The decoder path includes four convolutional layers that three of them are followed by a batch normalization. F: Filters.

1.3. Pearson's correlation coefficient regression (R_Regression)

Compute Pearson's r for each feature and the target. Pearson's r is also known as the Pearson correlation coefficient. Linear model for testing the individual effect of each of many regressors. This is a scoring function to be used in a feature selection procedure, not a free-standing feature selection procedure. The cross-correlation between each regressor and the target is computed as [6]:

$$E[(X[:, i] - mean(X[:, i])) * (y - mean(y))] / (std(X[:, i]) * std(y))$$

1.4.F-test for regression (F_Regression)\

Univariate linear regression tests returning F-statistic and p-values. Quick linear model for testing the effect of a single regressor, sequentially for many regressors. This is done in 2 steps: The cross correlation between each regressor and the target is computed using r_regression as:

$$E[(X[:, i] - mean(X[:, i])) * (y - mean(y))] / (std(X[:, i]) * std(y))$$

It is converted to an F score and then to a p-value. F_Regression is derived from R_Regression and will rank features in the same order if all the features are positively correlated with the target [7].

1.5. Principal Component Analysis (PCA)

PCA is a statistical unsupervised technique used in data analysis and Machine Learning (ML) to simplify the complexity of high-dimensional data while retaining most of the information. It works by identifying the directions, called principal components, along which the variability of the data is maximized. These components are orthogonal to each other and are derived from the eigenvectors of the data's covariance matrix, ranked according to their eigenvalues. In this study, PCA reduces the dimensionality by projecting the original data onto a smaller set of 10 significant components to prevent overfitting in ML prediction algorithm [8].

1.6. WeilBull Accelerated failure time (AFT)

Accelerated failure time (AFT) models are used widely in medical research, though to a much lesser extent than proportional hazards models. In an AFT model, the effect of covariates act to accelerate or decelerate the time to event of interest, that is, shorten or extend the time to event [9]. The Weibull model is a parametric survival model in which the outcome is assumed to follow a Weibull distribution. A unique property of the Weibull model is that when the accelerated failure time (AFT) assumption holds, the proportional hazards (PH) assumption also holds, making it compatible with both frameworks. In the PH formulation, the key assumption is that hazard ratios remain constant over time, whereas in the AFT formulation, survival times are assumed to accelerate or decelerate by a constant factor across covariate levels. This dual property is specific to the Weibull model and makes it especially useful in survival analysis [10].

1.7. Regression Algorithms (RA)

1.7.1. K-Nearest Neighbour

In supervised machine learning, the K-Nearest Neighbor (KNN) algorithm is a straightforward yet powerful technique for regression and classification. It works on the tenet that data points with comparable traits have a tendency to group together. KNN finds the 'K' nearest points (neighbors) in the training data when a new data point is added, and then assigns a value based on the average value for regression tasks or the majority class for classification tasks. The algorithm's non-parametric nature, which means it doesn't assume any particular distribution for the data points, is one of its advantages. This makes it adaptable to a variety of datasets. The performance of KNN is largely dependent on the value of 'K', the number of neighbors considered. An ideal 'K' balances the model's bias and variance to prevent overfitting or underfitting. Higher 'K' values produce more stable predictions because they analyze more data points and are less sensitive to noise. However, this can result in smoother decision boundaries, perhaps missing local nuances in the data. The approach relies on an appropriate distance measure, such as Euclidean or Manhattan distance, to locate the nearest neighbors [11].

1.7.2. AdaBoost Regressor (ABR)

Adaboost learning is a potent machine learning technique that enables the construction of highly accurate prediction models through the combination of multiple weak models. Adaboost, fundamentally, operates as an ensemble method wherein decision trees are iteratively trained to rectify the errors introduced by the preceding tree. By training each subsequent decision tree using the residuals of the previous tree, the model is able to evolve and develop gradually. The ultimate prognosis is computed by combining the predictions generated by each individual tree, assigning a weight to its accuracy-based contribution. This procedure enables Adaboost to effortlessly manage high-dimensional data and capture intricate interactions among features. In addition, built-in regularisation in Adaboost ensures that the model generalises well to new data and prevents overfitting. In general, Adaboost learning provides a resilient and adaptable approach for constructing accurate prediction models, rendering it a favoured option across an extensive variety of applications encompassing computer vision, natural language processing, and other domains [12].

1.7.3. Random Forest Regressor (RFR)

A Random Forest Regressor is a form of machine learning model that predicts continuous outcomes using a collection of decision trees. It is widely used in regression problems that aim to predict a numerical value due to its capability of managing complicated relationships among variables and delivering precise estimates of uncertainty. Similar to other ensemble methods, a Random Forest Regressor generates a final output by combining the predictions of multiple trees. A random subset of the training data and features is used to train each tree, and the final prediction is calculated by summing the outputs of all trees. The utilisation of randomness in the feature and data selection processes serves to mitigate overfitting and enhances the model's capacity to extrapolate to novel data. In addition, the model is robust against outliers and can accommodate absent values. Applications such as finance, marketing, and healthcare, where predicting continuous outcomes is crucial and the model's ability to provide accurate estimates of uncertainty is valuable, frequently employ Random Forest Regressors [13].

1.7.4. Multi-Layer Perceptron (MLPR)

For regression tasks, Multi-Layer Perceptron (MLP) regressors are a type of neural network. An MLP regressor, as compared to a linear regression model that operates under the assumption of a linear association between the input features and output variables, employs multiple layers of artificial neurons to discover non-linear relationships. An input layer, one or more concealed layers, and an output layer create the model. Every hidden layer is composed of a specific group of neurons. In turn, each neuron executes a computation on the inputs it receives from the previous layer and subsequently transmits the result to the neurons in the following layer. The final output is generated by applying an activation function to the output of the final hidden layer. One notable benefit of MLP regressors is their capacity to identify intricate patterns within datasets, which enables them to model non-linear associations between inputs and outputs with remarkable accuracy. They are frequently implemented in medical diagnosis, stock price prediction, and weather forecasting, among other applications. Nevertheless, MLP regressors are susceptible to overfitting, particularly when challenged with enormous datasets, and require precise hyperparameter optimisation in order to attain peak performance [14].

1.7.5. Decision Tree Regressor (DTR)

A Decision Tree Regressor is a form of machine learning model that predicts continuous outcomes using a tree-based structure. In contrast to the predefined categories employed by a conventional decision tree, a decision tree regressor generates predictions for continuous values, such as probabilities or prices. Based on the values of the input features, the model recursively divides the data into smaller subsets before fitting a statistical model, such as linear regression, to the data points within each subset. In order to arrive at the ultimate prediction, the tree is traversed from its root to each leaf node, where the predicted value is calculated using the attributes linked to that specific leaf node. When the relationships between the input features and the output variable are complex, decision tree regressors are beneficial; they can process both numeric and categorical features. In addition to being interpretable, which enables users to comprehend the methodology behind the model's predictions, these models are also applicable to classification and regression tasks. Nevertheless, decision tree regressors are susceptible to overfitting, which occurs

when the dataset contains an excessive number of irrelevant features; therefore, care must be taken to select the proper features and adjust the model's parameters [15].

1.7.6. Linear Regression (LR)

In machine learning, linear regression is a widely implemented algorithm employed for tasks involving the prediction of a continuous outcome variable from one or more input features. Linear regression is a statistical method that models the relationship between an output variable and input features through the use of a linear equation. The coefficients of the features are acquired through training with the data. The model operates under the assumption of a linear relationship between the output variable and the features, whereby any change in a feature results in a constant effect on the output variable, irrespective of the feature's level. As an algorithm for supervised learning, Linear Regression requires labelled training data in order to discover the connection between the input variable and the features. As a result of minimising the sum of squared differences between the predicted and actual values, the algorithm determines the linear equation that best describes the relationship between the output variable and the features. Linear regression is an exceptionally potent instrument used across many fields, including finance, economics, social sciences, and engineering, to predict continuous outcomes. Additionally, it provides an excellent basis for comprehending advanced algorithms in machine learning, including logistic regression and support vector machines [16].

1.7.7. Support Vector Machine (SVR)

For regression tasks, Support Vector Machine (SVM) regression is a type of machine learning algorithm. In contrast to conventional linear regression, which models the relationship between independent and dependent variables using a linear function, SVM regression maps inputs to outputs using a non-linear function. SVM regression operates on the principle of locating the hyperplane that divides the data points into distinct classes at the highest level possible. The objective of regression tasks is to identify the hyperplane where the mean squared error between the predicted and actual values is minimised. Support vector regression accomplishes this objective by optimising the margin separating the hyperplane from the closest data points. As the distance between the hyperplane and the support vectors, the margin signifies the model's robustness. A greater margin indicates an enhanced capacity of the model to

extrapolate to novel data. Support Vector Machine (SVM) regression proves to be highly advantageous when confronted with chaotic or unstructured data. Its usage extends across diverse domains, including finance, biology, and computer vision [17].

1.8. Hazard Ratio Survival Analysis (HRSA)

1.8.1. Fast Survival Support Vector Machines (FSSVM)

An expansion of the regular Support Vector Machine to right-censored time-to-event data is called a Survival Support Vector Machine. Its main benefit is that, with the use of the so-called kernel trick, it can take into account intricate, non-linear correlations between survival and attributes. The input features are implicitly mapped by a kernel function into high-dimensional feature spaces where a hyperplane can describe survival. Because of this, Survival Support Vector Machines may be applied to a large variety of data and are highly versatile [18].

1.8.2. Component-wise Gradient Boosting Survival Analysis (CWGBSA)

Gradient Boosting is a flexible framework for optimizing a variety of loss functions rather than a specific model. It builds a strong overall model by aggregating the predictions of several base learners, according to the strength in numbers concept. The base learners are sometimes known as weak learners since they are frequently relatively basic models that perform slightly better than random guessing. The predictions are combined additively, meaning that the addition of a base model improves the model as a whole [19].

1.8.3. Random Survival Forest (RSF)

An ensemble of tree-based learners makes up a Random Survival Forest, just like its well-known counterparts for regression and classification. By 1) generating each tree using a unique bootstrap sample of the original training data and 2) only evaluating the split criterion for a randomly chosen subset of features and thresholds at each node, a Random Survival Forest ensures that individual trees are de-correlated. The ensemble's predictions are created by adding up the predictions of each individual tree [20].

1.9.Pseudo-labeling

Pseudo-labeling [21] is a technique for semi-supervised learning, which is a type of ML that uses both labeled and unlabeled data. Pseudo-labeling works by using a model trained on labeled data to predict the labels for unlabeled data, and then using those "pseudo labels" to train the model in a supervised way on the unlabeled data. This can help improve the accuracy and generalization of the model, especially when there is not enough labeled data available. Of course, ultimately the performance of such a framework is tested on a fully labeled dataset.

2. Results
Supplemental Table S2. Results provided by regression algorithms (RA)

Dataset	<i>C</i> -	FSA	Algorit	SL	SL	SL R2	SSL	SSL	SSL R2	T-test p-
Dataset	Index	F SA	hm	<i>RMSE</i>	MAE	SL K2	<i>RMSE</i>	MAE	SSL KZ	value
CF	0.68	FR	KNN	1.41	1.07	0.00	1.52	1.19	-0.17	0.00
CF	0.68	RR	KNN	1.41	1.07	0.00	1.52	1.19	-0.17	0.00
CF	0.56	RR	ADB	1.42	1.09	-0.02	1.39	1.04	0.03	0.05
CF	0.68	FR	LRR	1.41	1.08	0.00	1.58	1.24	-0.25	0.13
CF	0.68	RR	LRR	1.41	1.08	0.00	1.58	1.24	-0.25	0.13
CF	0.68	FR	DTC	2.33	1.66	-1.73	1.79	1.37	-0.61	0.13
CF	0.68	RR	DTC	2.33	1.66	-1.73	1.79	1.37	-0.61	0.13
CF	0.68	FR	SVR	1.49	1.11	-0.11	1.53	1.21	-0.17	0.22
CF	0.68	RR	SVR	1.49	1.11	-0.11	1.53	1.21	-0.17	0.22
CF	0.68	FR	RFR	1.51	1.16	-0.14	1.54	1.21	-0.18	0.31
CF	0.68	RR	RFR	1.51	1.16	-0.14	1.54	1.21	-0.18	0.31
CF	0.68	FR	MLP	1.43	1.14	-0.02	1.53	1.21	-0.17	0.37
CF	0.68	RR	MLP	1.43	1.15	-0.02	1.46	1.16	-0.07	0.84
CF	0.64	FR	ADB	1.54	1.14	-0.19	1.47	1.13	-0.08	0.95
CT_DRF	0.70	FR	RFR	1.58	1.20	-0.25	9.02	3.62	-39.80	0.04

CT_DRF	0.70	FR	DTC	2.04	1.45	-1.08	8.79	3.71	-37.82	0.05
CT_DRF	0.65	FR	ADB	1.60	1.13	-0.28	1.49	1.03	-0.12	0.07
CT_DRF	0.50	RR	MLP	1.41	1.09	0.00	1.55	1.18	-0.21	0.07
CT_DRF	0.70	FR	SVR	1.54	1.15	-0.19	15.32	4.81	-116.84	0.09
CT_DRF	0.70	FR	LRR	2.73	1.65	-2.73	17.98	5.23	-161.17	0.11
CT_DRF	0.70	FR	MLP	1.79	1.38	-0.60	14.82	4.62	-109.19	0.11
CT_DRF	0.70	FR	KNN	1.52	1.16	-0.16	7.90	2.62	-30.31	0.18
CT_DRF	0.50	RR	ADB	1.41	1.06	0.00	1.41	1.09	0.00	0.26
CT_DRF	0.50	RR	LRR	1.41	1.08	0.00	1.49	1.10	-0.11	0.73
CT_DRF	0.50	RR	DTC	1.41	1.08	0.00	1.43	1.07	-0.02	0.73
CT_DRF	0.50	RR	RFR	1.41	1.09	0.00	1.47	1.07	-0.08	0.77
CT_DRF	0.50	RR	SVR	1.42	1.05	-0.02	1.44	1.06	-0.03	0.78
CT_DRF	0.50	RR	KNN	1.41	1.08	0.00	1.50	1.08	-0.12	0.95
CT_DRF+CF	0.65	FR	MLP	1.74	1.30	-0.52	1.60	1.13	-0.28	0.00
CT_DRF+CF	0.65	FR	RFR	1.58	1.12	-0.25	1.52	1.06	-0.16	0.12
CT_DRF+CF	0.50	RR	MLP	1.41	1.08	0.00	1.52	1.15	-0.17	0.19
CT_DRF+CF	0.50	RR	ADB	1.41	1.09	0.00	1.41	1.07	0.00	0.26
CT_DRF+CF	0.65	FR	LRR	1.63	1.18	-0.33	1.62	1.12	-0.32	0.45
CT_DRF+CF	0.65	FR	DTC	1.83	1.22	-0.67	1.69	1.13	-0.44	0.45
•										

CT_DRF+CF	0.65	FR	ADB	1.49	1.04	-0.11	1.54	1.07	-0.18	0.65
CT_DRF+CF	0.50	RR	LRR	1.41	1.08	0.00	1.49	1.10	-0.11	0.73
CT_DRF+CF	0.50	RR	DTC	1.41	1.08	0.00	1.43	1.07	-0.02	0.73
CT_DRF+CF	0.50	RR	RFR	1.41	1.09	0.00	1.47	1.07	-0.08	0.77
CT_DRF+CF	0.50	RR	SVR	1.42	1.05	-0.02	1.44	1.06	-0.03	0.78
CT_DRF+CF	0.65	FR	SVR	1.46	1.08	-0.08	1.53	1.09	-0.17	0.86
CT_DRF+CF	0.65	FR	KNN	1.50	1.10	-0.12	1.54	1.09	-0.19	0.91
CT_DRF+CF	0.50	RR	KNN	1.41	1.08	0.00	1.50	1.08	-0.12	0.95
$CT_DRF+CF+CT_HRF$	0.65	FR	MLP	1.80	1.31	-0.62	1.56	1.12	-0.22	0.02
$CT_DRF+CF+CT_HRF$	0.65	FR	RFR	1.58	1.12	-0.25	1.52	1.06	-0.16	0.12
$CT_DRF+CF+CT_HRF$	0.50	RR	ADB	1.41	1.08	0.00	1.41	1.07	0.00	0.26
$CT_DRF + CF + CT_HRF$	0.50	RR	MLP	1.41	1.09	0.00	1.49	1.13	-0.12	0.35
$CT_DRF+CF+CT_HRF$	0.65	FR	LRR	1.63	1.18	-0.33	1.62	1.12	-0.32	0.45
$CT_DRF+CF+CT_HRF$	0.65	FR	DTC	1.83	1.22	-0.67	1.69	1.13	-0.44	0.45
$CT_DRF + CF + CT_HRF$	0.65	FR	ADB	1.46	1.04	-0.08	1.45	1.02	-0.05	0.65
$CT_DRF+CF+CT_HRF$	0.50	RR	LRR	1.41	1.08	0.00	1.49	1.10	-0.11	0.73
$CT_DRF+CF+CT_HRF$	0.50	RR	DTC	1.41	1.08	0.00	1.43	1.07	-0.02	0.73
$CT_DRF+CF+CT_HRF$	0.50	RR	RFR	1.41	1.09	0.00	1.47	1.07	-0.08	0.77
$CT_DRF+CF+CT_HRF$	0.50	RR	SVR	1.42	1.05	-0.02	1.44	1.06	-0.03	0.78

CT_DRF+CF+CT_HRF	0.65	FR	SVR	1.46	1.08	-0.08	1.53	1.09	-0.17	0.86
$CT_DRF+CF+CT_HRF$	0.65	FR	KNN	1.50	1.10	-0.12	1.54	1.09	-0.19	0.91
$CT_DRF+CF+CT_HRF$	0.50	RR	KNN	1.41	1.08	0.00	1.50	1.08	-0.12	0.95
CT_DRF+CT_HRF	0.65	FR	MLP	1.76	1.30	-0.56	1.56	1.12	-0.22	0.03
$CT_DRF + CT_HRF$	0.65	FR	RFR	1.58	1.12	-0.25	1.52	1.06	-0.16	0.12
CT_DRF+CT_HRF	0.50	RR	MLP	1.41	1.08	0.00	1.53	1.15	-0.18	0.13
CT_DRF+CT_HRF	0.50	RR	ADB	1.41	1.08	0.00	1.41	1.07	0.00	0.26
$CT_DRF + CT_HRF$	0.65	FR	LRR	1.63	1.18	-0.33	1.62	1.12	-0.32	0.45
$CT_DRF + CT_HRF$	0.65	FR	DTC	1.83	1.22	-0.67	1.69	1.13	-0.44	0.45
$CT_DRF + CT_HRF$	0.50	RR	LRR	1.41	1.08	0.00	1.49	1.10	-0.11	0.73
$CT_DRF + CT_HRF$	0.50	RR	DTC	1.41	1.08	0.00	1.43	1.07	-0.02	0.73
CT_DRF+CT_HRF	0.50	RR	RFR	1.41	1.09	0.00	1.47	1.07	-0.08	0.77
$CT_DRF + CT_HRF$	0.50	RR	SVR	1.42	1.05	-0.02	1.44	1.06	-0.03	0.78
$CT_DRF + CT_HRF$	0.65	FR	ADB	1.60	1.12	-0.28	1.57	1.11	-0.24	0.85
CT_DRF+CT_HRF	0.65	FR	SVR	1.46	1.08	-0.08	1.53	1.09	-0.17	0.86
CT_DRF+CT_HRF	0.65	FR	KNN	1.50	1.10	-0.12	1.54	1.09	-0.19	0.91
CT_DRF+CT_HRF	0.50	RR	KNN	1.41	1.08	0.00	1.50	1.08	-0.12	0.95
CT_HRF	0.74	RR	KNN	1.41	1.09	0.00	1.49	1.21	-0.11	0.12
CT_HRF	0.61	FR	LRR	1.50	1.10	-0.13	1.47	1.05	-0.08	0.14

CT_HRF 0.74 RR SVR 1.77 1.41 -0.58 1.62 1.24 -0.31 0.24 CT_HRF 0.74 RR LRR 1.45 1.10 -0.06 1.60 1.20 -0.29 0.27 CT_HRF 0.59 RR ADB 1.50 1.13 -0.12 1.43 1.08 -0.03 0.28 CT_HRF 0.61 FR DTC 1.71 1.28 -0.47 1.62 1.16 -0.31 0.34 CT_HRF 0.61 FR ADB 1.41 1.02 0.01 1.47 1.08 -0.08 0.34 CT_HRF 0.61 FR ADB 1.41 1.02 0.01 1.47 1.08 -0.08 0.34 CT_HRF 0.61 FR MLP 1.50 1.11 -0.12 1.42 1.06 -0.01 0.37 CT_HRF 0.61 FR RFR 1.48 1.08 -0.11 1.54 1.13											
CT_HRF 0.59 RR ADB 1.50 1.13 -0.12 1.43 1.08 -0.03 0.28 CT_HRF 0.61 FR DTC 1.71 1.28 -0.47 1.62 1.16 -0.31 0.34 CT_HRF 0.61 FR ADB 1.41 1.02 0.01 1.47 1.08 -0.08 0.34 CT_HRF 0.74 RR DTC 1.47 1.10 -0.08 1.55 1.20 -0.20 0.37 CT_HRF 0.61 FR MLP 1.50 1.11 -0.12 1.42 1.06 -0.01 0.37 CT_HRF 0.61 FR RFR 1.48 1.08 -0.11 1.54 1.13 -0.19 0.43 CT_HRF 0.61 FR KNN 1.50 1.18 -0.12 1.50 1.14 -0.13 0.60 CT_HRF 0.74 RR MLP 1.51 1.12 -0.14 1.46 1.15	CT_HRF	0.74	RR	SVR	1.77	1.41	-0.58	1.62	1.24	-0.31	0.24
CT_HRF 0.61 FR DTC 1.71 1.28 -0.47 1.62 1.16 -0.31 0.34 CT_HRF 0.61 FR ADB 1.41 1.02 0.01 1.47 1.08 -0.08 0.34 CT_HRF 0.74 RR DTC 1.47 1.10 -0.08 1.55 1.20 -0.20 0.37 CT_HRF 0.61 FR MLP 1.50 1.11 -0.12 1.42 1.06 -0.01 0.37 CT_HRF 0.61 FR RFR 1.48 1.08 -0.11 1.54 1.13 -0.19 0.43 CT_HRF 0.61 FR RFR 1.48 1.08 -0.11 1.54 1.13 -0.19 0.43 CT_HRF 0.61 FR KNN 1.50 1.18 -0.12 1.50 1.14 -0.13 0.60 CT_HRF 0.74 RR RFR 1.54 1.21 -0.02 1.58 1.19	CT_HRF	0.74	RR	LRR	1.45	1.10	-0.06	1.60	1.20	-0.29	0.27
CT_HRF 0.61 FR ADB 1.41 1.02 0.01 1.47 1.08 -0.08 0.34 CT_HRF 0.74 RR DTC 1.47 1.10 -0.08 1.55 1.20 -0.20 0.37 CT_HRF 0.61 FR MLP 1.50 1.11 -0.12 1.42 1.06 -0.01 0.37 CT_HRF 0.61 FR RFR 1.48 1.08 -0.11 1.54 1.13 -0.19 0.43 CT_HRF 0.61 FR KNN 1.50 1.18 -0.12 1.50 1.14 -0.13 0.60 CT_HRF 0.61 FR KNN 1.50 1.18 -0.12 1.50 1.14 -0.13 0.60 CT_HRF 0.74 RR MLP 1.51 1.12 -0.14 1.46 1.15 -0.07 0.67 CT_HRF 0.61 FR SVR 1.45 1.07 -0.06 1.46 1.07	CT_HRF	0.59	RR	ADB	1.50	1.13	-0.12	1.43	1.08	-0.03	0.28
CT_HRF 0.74 RR DTC 1.47 1.10 -0.08 1.55 1.20 -0.20 0.37 CT_HRF 0.61 FR MLP 1.50 1.11 -0.12 1.42 1.06 -0.01 0.37 CT_HRF 0.61 FR RFR 1.48 1.08 -0.11 1.54 1.13 -0.19 0.43 CT_HRF 0.61 FR KNN 1.50 1.18 -0.12 1.50 1.14 -0.13 0.60 CT_HRF 0.74 RR MLP 1.51 1.12 -0.14 1.46 1.15 -0.07 0.67 CT_HRF 0.74 RR RFR 1.54 1.21 -0.20 1.58 1.19 -0.25 0.77 CT_HRF 0.61 FR SVR 1.45 1.07 -0.06 1.46 1.07 -0.07 0.89 CT_HRF+CF 0.74 RR LRR 1.48 1.17 -0.11 2.27 1.76	CT_HRF	0.61	FR	DTC	1.71	1.28	-0.47	1.62	1.16	-0.31	0.34
CT_HRF 0.61 FR MLP 1.50 1.11 -0.12 1.42 1.06 -0.01 0.37 CT_HRF 0.61 FR RFR 1.48 1.08 -0.11 1.54 1.13 -0.19 0.43 CT_HRF 0.61 FR KNN 1.50 1.18 -0.12 1.50 1.14 -0.13 0.60 CT_HRF 0.61 FR KNN 1.50 1.18 -0.12 1.50 1.14 -0.13 0.60 CT_HRF 0.74 RR MLP 1.51 1.12 -0.14 1.46 1.15 -0.07 0.67 CT_HRF 0.74 RR RFR 1.54 1.21 -0.20 1.58 1.19 -0.25 0.77 CT_HRF 0.61 FR SVR 1.45 1.07 -0.06 1.46 1.07 -0.07 0.89 CT_HRF+CF 0.74 RR MLP 1.48 1.17 -0.11 2.27 1.76	CT_HRF	0.61	FR	ADB	1.41	1.02	0.01	1.47	1.08	-0.08	0.34
CT_HRF 0.61 FR RFR 1.48 1.08 -0.11 1.54 1.13 -0.19 0.43 CT_HRF 0.61 FR KNN 1.50 1.18 -0.12 1.50 1.14 -0.13 0.60 CT_HRF 0.74 RR MLP 1.51 1.12 -0.14 1.46 1.15 -0.07 0.67 CT_HRF 0.74 RR RFR 1.54 1.21 -0.20 1.58 1.19 -0.25 0.77 CT_HRF 0.61 FR SVR 1.45 1.07 -0.06 1.46 1.07 -0.07 0.89 CT_HRF+CF 0.74 RR LRR 1.46 1.15 -0.06 1.86 1.50 -0.74 0.00 CT_HRF+CF 0.64 FR MLP 1.48 1.17 -0.11 2.27 1.76 -1.59 0.01 CT_HRF+CF 0.74 RR KNN 1.41 1.09 0.00 1.61 1.25<	CT_HRF	0.74	RR	DTC	1.47	1.10	-0.08	1.55	1.20	-0.20	0.37
CT_HRF 0.61 FR KNN 1.50 1.18 -0.12 1.50 1.14 -0.13 0.60 CT_HRF 0.74 RR MLP 1.51 1.12 -0.14 1.46 1.15 -0.07 0.67 CT_HRF 0.74 RR RFR 1.54 1.21 -0.20 1.58 1.19 -0.25 0.77 CT_HRF 0.61 FR SVR 1.45 1.07 -0.06 1.46 1.07 -0.07 0.89 CT_HRF+CF 0.74 RR LRR 1.46 1.15 -0.06 1.86 1.50 -0.74 0.00 CT_HRF+CF 0.64 FR MLP 1.48 1.17 -0.11 2.27 1.76 -1.59 0.01 CT_HRF+CF 0.74 RR SVR 1.52 1.11 -0.16 1.77 1.41 -0.57 0.02 CT_HRF+CF 0.74 RR KNN 1.44 1.11 -0.05 1.39 1	CT_HRF	0.61	FR	MLP	1.50	1.11	-0.12	1.42	1.06	-0.01	0.37
CT_HRF 0.74 RR MLP 1.51 1.12 -0.14 1.46 1.15 -0.07 0.67 CT_HRF 0.74 RR RFR 1.54 1.21 -0.20 1.58 1.19 -0.25 0.77 CT_HRF 0.61 FR SVR 1.45 1.07 -0.06 1.46 1.07 -0.07 0.89 CT_HRF+CF 0.74 RR LRR 1.46 1.15 -0.06 1.86 1.50 -0.74 0.00 CT_HRF+CF 0.64 FR MLP 1.48 1.17 -0.11 2.27 1.76 -1.59 0.01 CT_HRF+CF 0.74 RR SVR 1.52 1.11 -0.16 1.77 1.41 -0.57 0.02 CT_HRF+CF 0.64 FR KNN 1.41 1.09 0.00 1.61 1.25 -0.30 0.09 CT_HRF+CF 0.64 FR KNN 1.44 1.11 -0.05 1.39 <th< td=""><th>CT_HRF</th><td>0.61</td><td>FR</td><td>RFR</td><td>1.48</td><td>1.08</td><td>-0.11</td><td>1.54</td><td>1.13</td><td>-0.19</td><td>0.43</td></th<>	CT_HRF	0.61	FR	RFR	1.48	1.08	-0.11	1.54	1.13	-0.19	0.43
CT_HRF 0.74 RR RFR 1.54 1.21 -0.20 1.58 1.19 -0.25 0.77 CT_HRF 0.61 FR SVR 1.45 1.07 -0.06 1.46 1.07 -0.07 0.89 CT_HRF+CF 0.74 RR LRR 1.46 1.15 -0.06 1.86 1.50 -0.74 0.00 CT_HRF+CF 0.64 FR MLP 1.48 1.17 -0.11 2.27 1.76 -1.59 0.01 CT_HRF+CF 0.74 RR SVR 1.52 1.11 -0.16 1.77 1.41 -0.57 0.02 CT_HRF+CF 0.74 RR KNN 1.41 1.09 0.00 1.61 1.25 -0.30 0.09 CT_HRF+CF 0.64 FR KNN 1.44 1.11 -0.05 1.39 1.02 0.04 0.09 CT_HRF+CF 0.74 RR RFR 1.56 1.22 -0.22 1.81 <	CT_HRF	0.61	FR	KNN	1.50	1.18	-0.12	1.50	1.14	-0.13	0.60
CT_HRF 0.61 FR SVR 1.45 1.07 -0.06 1.46 1.07 -0.07 0.89 CT_HRF+CF 0.74 RR LRR 1.46 1.15 -0.06 1.86 1.50 -0.74 0.00 CT_HRF+CF 0.64 FR MLP 1.48 1.17 -0.11 2.27 1.76 -1.59 0.01 CT_HRF+CF 0.74 RR SVR 1.52 1.11 -0.16 1.77 1.41 -0.57 0.02 CT_HRF+CF 0.74 RR KNN 1.41 1.09 0.00 1.61 1.25 -0.30 0.09 CT_HRF+CF 0.64 FR KNN 1.44 1.11 -0.05 1.39 1.02 0.04 0.09 CT_HRF+CF 0.74 RR RFR 1.56 1.22 -0.22 1.81 1.40 -0.64 0.19	CT_HRF	0.74	RR	MLP	1.51	1.12	-0.14	1.46	1.15	-0.07	0.67
CT_HRF+CF 0.74 RR LRR 1.46 1.15 -0.06 1.86 1.50 -0.74 0.00 CT_HRF+CF 0.64 FR MLP 1.48 1.17 -0.11 2.27 1.76 -1.59 0.01 CT_HRF+CF 0.74 RR SVR 1.52 1.11 -0.16 1.77 1.41 -0.57 0.02 CT_HRF+CF 0.74 RR KNN 1.41 1.09 0.00 1.61 1.25 -0.30 0.09 CT_HRF+CF 0.64 FR KNN 1.44 1.11 -0.05 1.39 1.02 0.04 0.09 CT_HRF+CF 0.74 RR RFR 1.56 1.22 -0.22 1.81 1.40 -0.64 0.19	CT_HRF	0.74	RR	RFR	1.54	1.21	-0.20	1.58	1.19	-0.25	0.77
CT_HRF+CF 0.64 FR MLP 1.48 1.17 -0.11 2.27 1.76 -1.59 0.01 CT_HRF+CF 0.74 RR SVR 1.52 1.11 -0.16 1.77 1.41 -0.57 0.02 CT_HRF+CF 0.74 RR KNN 1.41 1.09 0.00 1.61 1.25 -0.30 0.09 CT_HRF+CF 0.64 FR KNN 1.44 1.11 -0.05 1.39 1.02 0.04 0.09 CT_HRF+CF 0.74 RR RFR 1.56 1.22 -0.22 1.81 1.40 -0.64 0.19	CT_HRF	0.61	FR	SVR	1.45	1.07	-0.06	1.46	1.07	-0.07	0.89
CT_HRF+CF 0.74 RR SVR 1.52 1.11 -0.16 1.77 1.41 -0.57 0.02 CT_HRF+CF 0.74 RR KNN 1.41 1.09 0.00 1.61 1.25 -0.30 0.09 CT_HRF+CF 0.64 FR KNN 1.44 1.11 -0.05 1.39 1.02 0.04 0.09 CT_HRF+CF 0.74 RR RFR 1.56 1.22 -0.22 1.81 1.40 -0.64 0.19	CT_HRF+CF	0.74	RR	LRR	1.46	1.15	-0.06	1.86	1.50	-0.74	0.00
CT_HRF+CF 0.74 RR KNN 1.41 1.09 0.00 1.61 1.25 -0.30 0.09 CT_HRF+CF 0.64 FR KNN 1.44 1.11 -0.05 1.39 1.02 0.04 0.09 CT_HRF+CF 0.74 RR RFR 1.56 1.22 -0.22 1.81 1.40 -0.64 0.19	CT_HRF+CF	0.64	FR	MLP	1.48	1.17	-0.11	2.27	1.76	-1.59	0.01
CT_HRF+CF 0.64 FR KNN 1.44 1.11 -0.05 1.39 1.02 0.04 0.09 CT_HRF+CF 0.74 RR RFR 1.56 1.22 -0.22 1.81 1.40 -0.64 0.19	CT_HRF+CF	0.74	RR	SVR	1.52	1.11	-0.16	1.77	1.41	-0.57	0.02
CT_HRF+CF 0.74 RR RFR 1.56 1.22 -0.22 1.81 1.40 -0.64 0.19	CT_HRF+CF	0.74	RR	KNN	1.41	1.09	0.00	1.61	1.25	-0.30	0.09
	CT_HRF+CF	0.64	FR	KNN	1.44	1.11	-0.05	1.39	1.02	0.04	0.09
CT_HRF+CF 0.64 FR ADB 1.55 1.17 -0.21 1.49 1.08 -0.11 0.20	CT_HRF+CF	0.74	RR	RFR	1.56	1.22	-0.22	1.81	1.40	-0.64	0.19
	CT_HRF+CF	0.64	FR	ADB	1.55	1.17	-0.21	1.49	1.08	-0.11	0.20

CT_HRF+CF	0.64	FR	SVR	1.43	1.06	-0.03	1.42	1.05	-0.01	0.24
CT_HRF+CF	0.74	RR	MLP	1.45	1.12	-0.05	1.49	1.20	-0.11	0.29
CT_HRF+CF	0.64	FR	DTC	1.57	1.15	-0.23	1.46	1.08	-0.07	0.45
CT_HRF+CF	0.64	FR	LRR	1.50	1.10	-0.13	1.48	1.08	-0.09	0.68
CT_HRF+CF	0.64	FR	RFR	1.46	1.08	-0.06	1.49	1.07	-0.12	0.92
CT_HRF+CF	0.74	RR	DTC	1.69	1.34	-0.44	2.00	1.36	-1.01	0.92
CT_HRF+CF	0.59	RR	ADB	1.47	1.10	-0.08	1.46	1.10	-0.08	0.96
PET_DRF	0.66	FR	RFR	1.32	1.02	0.12	1.73	1.23	-0.50	0.04
PET_DRF	0.66	FR	SVR	1.43	1.07	-0.02	1.49	1.13	-0.11	0.14
PET_DRF	0.50	RR	RFR	1.41	1.09	0.00	1.41	1.07	0.00	0.26
PET_DRF	0.50	RR	LRR	1.41	1.08	0.00	1.41	1.07	0.00	0.26
PET_DRF	0.50	RR	ADB	1.41	1.08	0.00	1.41	1.07	0.00	0.26
PET_DRF	0.66	FR	KNN	1.46	1.12	-0.07	1.62	1.20	-0.32	0.30
PET_DRF	0.66	FR	ADB	1.33	1.01	0.11	1.71	1.14	-0.47	0.31
PET_DRF	0.50	RR	DTC	1.41	1.08	0.00	1.42	1.06	-0.01	0.33
PET_DRF	0.66	FR	DTC	1.59	1.13	-0.27	1.96	1.31	-0.93	0.34
PET_DRF	0.50	RR	KNN	1.41	1.08	0.00	1.42	1.05	-0.02	0.38
PET_DRF	0.66	FR	MLP	1.45	1.14	-0.06	1.41	1.08	0.01	0.54
PET_DRF	0.66	FR	LRR	1.49	1.09	-0.11	1.59	1.14	-0.27	0.54

PET_DRF	0.50	RR	MLP	1.41	1.09	0.00	1.48	1.10	-0.09	0.74
PET_DRF	0.50	RR	SVR	1.42	1.05	-0.02	1.42	1.05	-0.02	
PET_DRF+CF	0.67	FR	RFR	1.32	1.02	0.13	1.59	1.17	-0.27	0.08
PET_DRF+CF	0.67	FR	SVR	1.43	1.07	-0.02	1.49	1.12	-0.11	0.22
PET_DRF+CF	0.50	RR	ADB	1.42	1.10	-0.01	1.41	1.06	0.00	0.26
PET_DRF+CF	0.50	RR	RFR	1.41	1.09	0.00	1.41	1.07	0.00	0.26
PET_DRF+CF	0.50	RR	LRR	1.41	1.08	0.00	1.41	1.07	0.00	0.26
PET_DRF+CF	0.67	FR	DTC	1.57	1.11	-0.24	1.83	1.28	-0.68	0.31
PET_DRF+CF	0.50	RR	DTC	1.41	1.08	0.00	1.42	1.06	-0.01	0.33
PET_DRF+CF	0.67	FR	MLP	1.48	1.20	-0.11	1.40	1.10	0.02	0.36
PET_DRF+CF	0.50	RR	KNN	1.41	1.08	0.00	1.42	1.05	-0.02	0.38
PET_DRF+CF	0.67	FR	ADB	1.36	1.03	0.07	1.56	1.12	-0.21	0.49
PET_DRF+CF	0.67	FR	LRR	1.48	1.09	-0.10	1.57	1.12	-0.24	0.50
PET_DRF+CF	0.50	RR	MLP	1.41	1.09	0.00	1.49	1.10	-0.12	0.63
PET_DRF+CF	0.67	FR	KNN	1.46	1.12	-0.06	1.50	1.13	-0.13	0.81
PET_DRF+CF	0.50	RR	SVR	1.42	1.05	-0.02	1.42	1.05	-0.02	
$PET_DRF+CF+PET_HRF$	0.66	FR	MLP	1.49	1.21	-0.12	2.98	2.55	-3.45	0.00
$PET_DRF+CF+PET_HRF$	0.66	FR	ADB	1.51	1.12	-0.14	1.90	1.36	-0.82	0.07
PET_DRF+CF+PET_HRF	0.66	FR	RFR	1.43	1.12	-0.03	1.70	1.26	-0.45	0.17

PET_DRF+CF+PET_HRF	0.50	RR	RFR	1.41	1.09	0.00	1.41	1.07	0.00	0.26
PET_DRF+CF+PET_HRF	0.50	RR	LRR	1.41	1.08	0.00	1.41	1.07	0.00	0.26
$PET_DRF+CF+PET_HRF$	0.50	RR	ADB	1.41	1.08	0.00	1.41	1.07	0.00	0.26
$PET_DRF+CF+PET_HRF$	0.66	FR	DTC	1.83	1.35	-0.67	2.26	1.60	-1.57	0.29
$PET_DRF+CF+PET_HRF$	0.50	RR	DTC	1.41	1.08	0.00	1.42	1.06	-0.01	0.33
PET_DRF+CF+PET_HRF	0.50	RR	KNN	1.41	1.08	0.00	1.42	1.05	-0.02	0.38
$PET_DRF+CF+PET_HRF$	0.66	FR	LRR	1.50	1.16	-0.13	1.65	1.20	-0.36	0.60
PET_DRF+CF+PET_HRF	0.50	RR	MLP	1.41	1.09	0.00	1.48	1.10	-0.11	0.69
PET_DRF+CF+PET_HRF	0.66	FR	KNN	1.52	1.18	-0.17	1.53	1.21	-0.17	0.75
PET_DRF+CF+PET_HRF	0.66	FR	SVR	1.42	1.07	-0.01	1.40	1.07	0.01	0.87
$PET_DRF+CF+PET_HRF$	0.50	RR	SVR	1.42	1.05	-0.02	1.42	1.05	-0.02	
PET_DRF+PET_HRF	0.50	RR	RFR	1.41	1.09	0.00	1.41	1.07	0.00	0.26
PET_DRF+PET_HRF	0.50	RR	LRR	1.41	1.08	0.00	1.41	1.07	0.00	0.26
PET_DRF+PET_HRF	0.50	RR	ADB	1.41	1.08	0.00	1.41	1.07	0.00	0.26
PET_DRF+PET_HRF	0.50	RR	DTC	1.41	1.08	0.00	1.42	1.06	-0.01	0.33
PET_DRF+PET_HRF	0.50	RR	KNN	1.41	1.08	0.00	1.42	1.05	-0.02	0.38
PET_DRF+PET_HRF	0.66	FR	MLP	1.42	1.14	-0.02	1.44	1.18	-0.03	0.58
PET_DRF+PET_HRF	0.50	RR	MLP	1.41	1.09	0.00	1.48	1.10	-0.10	0.67
PET_DRF+PET_HRF	0.66	FR	LRR	1.51	1.15	-0.14	1.52	1.17	-0.17	0.71

PET_DRF+PET_HRF	0.66	FR	ADB	1.46	1.13	-0.07	1.46	1.15	-0.07	0.75
PET_DRF+PET_HRF	0.66	FR	SVR	1.42	1.09	-0.01	1.41	1.08	0.00	0.79
PET_DRF+PET_HRF	0.66	FR	RFR	1.45	1.17	-0.06	1.53	1.18	-0.17	0.91
$PET_DRF + PET_HRF$	0.66	FR	KNN	1.47	1.14	-0.08	1.49	1.14	-0.11	0.95
$PET_DRF + PET_HRF$	0.66	FR	DTC	1.74	1.36	-0.53	2.69	1.37	-2.62	0.98
$PET_DRF + PET_HRF$	0.50	RR	SVR	1.42	1.05	-0.02	1.42	1.05	-0.02	
PET_HRF	0.63	FR	MLP	2.17	1.79	-1.36	1.42	1.10	-0.02	0.00
PET_HRF	0.63	FR	ADB	1.57	1.20	-0.23	1.38	1.05	0.04	0.00
PET_HRF	0.68	RR	SVR	137.64	58.33	-9507.08	1.37	1.04	0.06	0.00
PET_HRF	0.63	FR	RFR	1.59	1.25	-0.27	1.47	1.13	-0.09	0.00
PET_HRF	0.63	FR	DTC	1.80	1.39	-0.63	1.51	1.11	-0.14	0.03
PET_HRF	0.68	RR	KNN	1.53	1.20	-0.18	1.43	1.07	-0.03	0.11
PET_HRF	0.63	FR	SVR	1.42	1.07	-0.01	1.39	1.05	0.03	0.22
PET_HRF	0.63	FR	LRR	1.48	1.13	-0.09	1.50	1.17	-0.12	0.43
PET_HRF	0.63	FR	KNN	1.52	1.16	-0.15	1.44	1.12	-0.04	0.52
PET_HRF	0.68	RR	RFR	1.58	1.23	-0.25	1.54	1.20	-0.18	0.66
PET_HRF	0.68	RR	DTC	1.70	1.29	-0.45	1.77	1.34	-0.57	0.70
PET_HRF	0.63	RR	ADB	1.52	1.14	-0.16	1.46	1.12	-0.08	0.71
PET_HRF	0.68	RR	LRR	1.50	1.14	-0.13	1.49	1.15	-0.12	0.75

PET_HRF	0.68	RR	MLP	1.45	1.06	-0.06	1.37	1.08	0.06	0.85
PET_HRF+CF	0.67	RR	SVR	100.18	42.79	-5035.65	1.48	1.16	-0.10	0.00
PET_HRF+CF	0.63	FR	DTC	1.80	1.39	-0.63	1.45	1.08	-0.06	0.01
PET_HRF+CF	0.63	FR	RFR	1.58	1.23	-0.25	1.49	1.14	-0.11	0.04
PET_HRF+CF	0.67	RR	DTC	1.67	1.25	-0.40	2.07	1.57	-1.15	0.08
PET_HRF+CF	0.67	RR	MLP	1.42	1.11	-0.02	1.47	1.18	-0.09	0.24
PET_HRF+CF	0.63	RR	ADB	1.51	1.14	-0.15	1.45	1.11	-0.06	0.39
PET_HRF+CF	0.63	FR	KNN	1.51	1.14	-0.14	1.44	1.09	-0.04	0.40
PET_HRF+CF	0.63	FR	LRR	1.50	1.14	-0.13	1.43	1.10	-0.02	0.56
PET_HRF+CF	0.63	FR	SVR	1.42	1.06	-0.01	1.41	1.05	0.00	0.63
PET_HRF+CF	0.63	FR	MLP	1.41	1.05	0.00	1.43	1.07	-0.02	0.65
PET_HRF+CF	0.67	RR	KNN	1.53	1.20	-0.18	1.50	1.17	-0.12	0.71
PET_HRF+CF	0.63	FR	ADB	1.48	1.09	-0.10	1.46	1.10	-0.07	0.89
PET_HRF+CF	0.67	RR	RFR	1.56	1.21	-0.22	1.56	1.21	-0.23	0.96
PET_HRF+CF	0.67	RR	LRR	1.49	1.15	-0.12	1.52	1.15	-0.16	0.96

HRF: handcrafted Radiomics features, DRF: deep Radiomics features, DRF_CT: DRFs extracted from segmented CT, DRF_PET: DRFs extracted from segmented PET, HRF_CT: HFRs extracted from segmented CT, HRF_PET: HFRs extracted from segmented PET, FFCV: Five-Fold Cross-Validation, SSL: Semi-supervised Learning, SL: Supervised Learning, MAE: Mean Absolute Error, STD: Standard Deviation, ABR: AdaBoost Regressor, RFR: Random Forest Regressor, MLPR: Multi-Layer Perceptron Regressor, DTR: Decision Tree Regressor, LR: Linear Regression, SVR: Support Vector Machine Regressor, KNNR: K-Nearest Neighbor Regressor.

Supplemental Table S3. Top 10 features and parameters of top results

Dataset	FSA	Algorit	SL_Top10_Features	SL_BestP	SSL_Top10_Features	SSL_Best
		hm		arams		Params
PET_HR	FR	ADB	cm_joint_max_3D_comb (0.0890),	{'learning	szm_szhge_3D (0.2486),	{'learning
F			szm_zsnu_norm_3D (0.0767),	_rate':	cm_joint_max_3D_avg (0.0885),	_rate':
			szm_szhge_3D (0.0078),	0.1, 'loss':	cm_energy_3D_comb (0.0670),	0.01,
			cm_joint_max_3D_avg (0.0007),	'linear',	cm_joint_max_3D_comb (0.0623),	'loss':
			cm_energy_3D_comb (0.0000),	'n_estima	szm_zsnu_norm_3D (0.0515),	'square',
			szm_sze_3D (0.0000),	tors': 10}	szm_sze_3D (0.0502), morph_moran_i	'n_estimat
			cm_energy_3D_avg (0.0000),		(0.0268), morph_geary_c (0.0157),	ors': 10}
			cm_joint_entr_3D_avg (0.0000),		cm_energy_3D_avg (0.0039),	
			morph_geary_c (0.0000), morph_moran_i		cm_joint_entr_3D_avg (0.0000)	
			(0.0000)			
CF	RR	ADB	ageatdiagnosis (0.0761), FBase (0.0236),	{'learning	Wt_loss_c (0.1122), ageatdiagnosis	{'learning
			Wt_loss_c (0.0140),	_rate':	(0.1086), Correct_baseline_ECOG	_rate':
			Correct_baseline_ECOG (0.0114),	0.1, 'loss':	(0.0849), Sex (0.0697), Recurrence_status	0.1, 'loss':
			Fractionation_cat (0.0077),	'square',	(0.0402), Met_no0_yes1 (0.0381), FBase	'square',
			Met_no0_yes1 (0.0000), Sex (0.0000),	'n_estima	(0.0198), Fractionation_cat (0.0156),	'n_estimat
			Recurrence_status (0.0000),	tors': 10}		ors': 10}

			chemotherapy (0.0000),		chemotherapy (0.0125),	
			PostOpResidualTumourSx1 (0.0000)		PostOpResidualTumourSx1 (0.0034)	
CT_DRF	FR	ADB	459 (0.6831), 505 (0.2896), 298 (0.0926),	{'learning	298 (0.2403), 114 (0.1455), 480 (0.1076),	{'learning
			114 (0.0919), 456 (0.0292), 291 (0.0287),	_rate':	427 (0.0481), 461 (0.0361), 459 (0.0192),	_rate':
			480 (0.0282), 427 (0.0098), 420 (0.0038),	0.01,	291 (0.0107), 420 (0.0080), 505 (0.0000),	0.01,
			461 (0.0000)	'loss':	456 (0.0000)	'loss':
				'linear',		'linear',
				'n_estima		'n_estimat
				tors': 10}		ors': 10}
PET_DR	FR	RFR	DF327 (0.6999), DF330 (0.6497), DF2	{'max_de	DF2 (0.2547), DF863 (0.2515), DF816	{'max_de
F+CF			(0.1416), DF816 (0.1125), DF586	pth': 5,	(0.1715), DF58 (0.1071), DF98 (0.0538),	pth': 5,
			(0.0967), DF98 (0.0655), DF58 (0.0483),	'n_estima	DF330 (0.0140), DF327 (0.0086), DF212	'n_estimat
			DF625 (0.0370), DF212 (0.0204), DF863	tors':	(0.0078), DF625 (0.0058), DF586 (0.0037)	ors': 50}
			(0.0106)	100}		
CT+CF	FR	KNN	Smoking Pack Years (0.3584),	{'algorith	Smoking Pack Years (0.2774),	{'algorith
			Smoking_cat (0.0179), dzm_sdlge_3D	m': 'auto',	Smoking_cat (0.1100), ngl_lde_3D	m': 'auto',
			(0.0010), szm_lgze_3D (0.0004),	'n_neighb	(0.0238), morph_av (0.0237),	'n_neighb
			morph_av (0.0000), ngl_lde_3D (0.0000),	ors': 7,	dzm_sdlge_3D (0.0054), szm_lgze_3D	ors': 9,
			szm_szlge_3D (0.0000), dzm_lgze_3D		(0.0049), dzm_lgze_3D (0.0049),	

			(0.0000), ngl_dcnu_norm_3D (0.0000),	'weights':	ngl_dcnu_norm_3D (0.0046),	'weights':
			ngl_ldlge_3D (0.0000)	'uniform'}	szm_szlge_3D (0.0029), ngl_ldlge_3D	'uniform'}
					(0.0005)	
PET_DR	FR	ADB	DF241 (0.1918), DF277 (0.1293), DF98	{'learning	DF2 (0.1790), DF863 (0.1503), DF277	{'learning
F			(0.1013), DF58 (0.0814), DF863	_rate':	(0.1022), DF58 (0.0865), DF241 (0.0693),	_rate':
			(0.0705), DF2 (0.0319), DF625 (0.0000),	0.1, 'loss':	DF98 (0.0170), DF212 (0.0069), DF625	0.01,
			DF330 (0.0000), DF586 (0.0000), DF212	'linear',	(0.0000), DF586 (0.0000), DF330 (0.0000)	'loss':
			(0.0000)	'n_estima		'linear',
				tors': 10}		'n_estimat
						ors': 10}
CT	FR	ADB	dzm_sdlge_3D (0.3624), morph_av	{'learning	szm_szlge_3D (0.1629), dzm_sdlge_3D	{'learning
			(0.1769), cm_info_corr1_3D_avg	_rate':	(0.0894), ngl_ldlge_3D (0.0566),	_rate':
			(0.0956), stat_qcod (0.0897),	0.01,	cm_info_corr1_3D_avg (0.0533),	0.01,
			dzm_lgze_3D (0.0175), ngl_hdhge_3D	'loss':	stat_qcod (0.0487), szm_lgze_3D (0.0201),	'loss':
			(0.0000), ngl_ldlge_3D (0.0000),	'square',	morph_av (0.0199),	'square',
			szm_szlge_3D (0.0000), szm_lgze_3D	'n_estima	cm_info_corr2_3D_avg (0.0051),	'n_estimat
			(0.0000), cm_info_corr2_3D_avg	tors': 10}	ngl_hdhge_3D (0.0019), dzm_lgze_3D	ors': 10}
			(0.0000)		(0.0006)	

PET_DR	RR	KNN	DF1020 (0.0000), DF1012 (0.0000),	{'algorith	DF1020 (0.0000), DF1012 (0.0000),	{'algorith
F+CF+P			DF1006 (0.0000), DF1001 (0.0000),	m':	DF1006 (0.0000), DF1001 (0.0000),	m': 'auto',
ET_HRF			DF991 (0.0000), DF988 (0.0000), DF977	'ball_tree'	DF991 (0.0000), DF988 (0.0000), DF977	'n_neighb
			(0.0000), DF965 (0.0000), DF948	,	(0.0000), DF965 (0.0000), DF948	ors': 3,
			(0.0000), DF928 (0.0000)	'n_neighb	(0.0000), DF928 (0.0000)	'weights':
				ors': 3,		'uniform'}
				'weights':		
				'uniform'}		
PET_DR	RR	KNN	DF1020 (0.0000), DF1012 (0.0000),	{'algorith	DF1020 (0.0000), DF1012 (0.0000),	{'algorith
$F+PET_{-}$			DF1006 (0.0000), DF1001 (0.0000),	m':	DF1006 (0.0000), DF1001 (0.0000),	m': 'auto',
HRF			DF991 (0.0000), DF988 (0.0000), DF977	'ball_tree'	DF991 (0.0000), DF988 (0.0000), DF977	'n_neighb
			(0.0000), DF965 (0.0000), DF948	,	(0.0000), DF965 (0.0000), DF948	ors': 3,
			(0.0000), DF928 (0.0000)	'n_neighb	(0.0000), DF928 (0.0000)	'weights':
				ors': 3,		'uniform'}
				'weights':		
				'uniform'}		
PET_HR	FR	SVR	szm_szhge_3D (0.1071), dzm_sdhge_3D	{'C': 1,	szm_szhge_3D (0.1343), dzm_sdhge_3D	{'C': 1,
F+CF			(0.0399), Smoking_cat (0.0064),	'degree':	(0.1128), Smoking_cat (0.0064),	'degree':
			ngl_glnu_norm_3D (0.0000),	3,	morph_geary_c (0.0000), morph_moran_i	

			cm_joint_max_3D_comb (0.0000),	'kernel':	(0.0000), cm_joint_max_3D_comb	3, 'kernel':
			morph_geary_c (0.0000),	'rbf'}	(0.0000), cm_joint_max_3D_avg (0.0000),	'rbf'}
			cm_joint_max_3D_avg (0.0000),	,	ngl_glnu_norm_3D (0.0000),	,
			cm_energy_3D_comb (0.0000),		cm_energy_3D_comb (0.0000),	
			cm_energy_3D_avg (0.0000), morph_moran_i (0.0000)		cm_energy_3D_avg (0.0000)	
CT_DRF	FR	ADB	DF459 (0.2402), DF505 (0.1674), DF114	{'learning	DF298 (0.2844), DF427 (0.1225), DF114	{'learning
+CF			(0.1316), DF456 (0.1215), DF480	_rate':	(0.0941), DF480 (0.0779), DF505	_rate':
			(0.0518), DF291 (0.0206), DF427	0.1, 'loss':	(0.0255), DF459 (0.0247), DF456	0.1, 'loss':
			(0.0192), DF420 (0.0190), DF461	'linear',	(0.0002), DF461 (0.0000), DF420	'linear',
			(0.0010), DF298 (0.0009)	'n_estima	(0.0000), DF291 (0.0000)	'n_estimat
				tors': 10}		ors': 10}
CT_DRF	FR	ADB	DF459 (0.1361), DF456 (0.1087), DF480	{'learning	DF298 (0.2480), DF427 (0.1489), DF114	{'learning
+CF+CT			(0.0974), DF291 (0.0683), DF461	_rate':	(0.0636), DF459 (0.0429), DF480	_rate':
_HRF			(0.0362), DF298 (0.0131), DF114	0.01,	(0.0391), DF420 (0.0183), DF461	0.01,
			(0.0097), DF427 (0.0083), DF420	'loss':	(0.0161), DF291 (0.0157), DF456	'loss':
			(0.0074), DF505 (0.0000)	'square',	(0.0144), DF505 (0.0090)	'linear',
				'n_estima		'n_estimat
				tors': 10}		ors': 10}

CT_DRF	RR	SVR	DF1012 (0.0000), DF884 (0.0000),	{'C': 0.01,	DF505 (0.1062), DF459 (0.0769), DF179	{'C': 1,
+ <i>CT_HR</i>			DF756 (0.0000), DF684 (0.0000), DF663	'degree':	(0.0707), DF684 (0.0631), DF510	'degree':
F			(0.0000), DF628 (0.0000), DF535	2,	(0.0596), DF502 (0.0448), DF480	2, 'kernel':
			(0.0000), DF510 (0.0000), DF507	'kernel':	(0.0446), DF473 (0.0445), DF246	'linear'}
			(0.0000), DF505 (0.0000)	'linear'}	(0.0233), DF462 (0.0195)	

HRF: handcrafted Radiomics features, DRF: deep Radiomics features, DRF_CT: DRFs extracted from segmented CT, DRF_PET: DRFs extracted from segmented PET, HRF_CT: HFRs extracted from segmented CT, HRF_PET: HFRs extracted from segmented PET, FFCV: Five-Fold Cross-Validation, SSL: Semi-supervised Learning, SL: Supervised Learning, MAE: Mean Absolute Error, STD: Standard Deviation, ABR: AdaBoost Regressor, RFR: Random Forest Regressor, SVR: Support Vector Machine Regressor, KNNR: K-Nearest Neighbor Regressor, FSA: Feature selection Algorithm, RR: r_regression, FR: f_regression.

Supplemental Table S4. A list of the most important radiomics features used in this study, detailing their abbreviated names, full descriptions, and corresponding categories

Abbreviation	Complete Form	Category	Description
ngt_strength_3D	Neighbouring Grey Tone Difference	Texture	Measures the primitiveness of the texture. High
	Matrix (NGTDM) Strength		strength means high contrast.
ngt_coarseness_3D	NGTDM Coarseness	Texture	Measures the spatial rate of change in intensity.
			Lower values mean "finer" texture.

dzm_sdhge_3D	Dependent Zone Matrix (DZM)	Texture	Measures the joint distribution of small dependence
	Small Dependence High Grey Level		zones with high grey levels.
	Emphasis		
dzm_zdnu_norm_3D	DZM Zone Distance Non-	Texture	Measures the variability of zone distances in the
	Uniformity Normalized		image, normalized.
dzm_hgze_3D	DZM High Grey Level Zone	Texture	Measures the distribution of high grey-level values.
	Emphasis		
szm_szhge_3D	Size Zone Matrix (SZM) Small Zone	Texture	Measures the joint distribution of small size zones
	High Grey Level Emphasis		with high grey levels.
szm_zsnu_norm_3D	SZM Zone Size Non-Uniformity	Texture	Measures the variability of zone sizes in the image,
	Normalized		normalized.
szm_sze_3D	SZM Small Zone Emphasis	Texture	Measures the distribution of small size zones.
cm_joint_max_3D_avg	Co-occurrence Matrix (GLCM) Joint	Texture	Measures the most predominant pair of neighbouring
	Maximum		intensity values.
cm_joint_entr_3D_avg	Co-occurrence Matrix (GLCM) Joint	Texture	Measures the randomness/complexity of the intensity
	Entropy		distribution.
cm_energy_3D_avg	Co-occurrence Matrix (GLCM)	Texture	Measures the textural uniformity (also called Angular
	Energy		Second Moment).

ivh_diff_v10_v90	Intensity-Volume Histogram (IVH)	Intensity	The range of intensity values containing the central
	Difference between V10 and V90		80% of the tumor volume.
ivh_v10	IVH Intensity at 10th Volume	Intensity	The intensity level below which 10% of the tumor
	Percentile		volume exists.
morph_geary_c	Morphological Geary's C	Shape	Measures spatial autocorrelation; how similar a voxel
			is to its neighbors.
morph_av	Morphological Feature (Average)	Shape	This is not a standard feature name. 'morph' refers to
			shape, and 'av' likely means an average of some
			property, but the specific feature is unclear.

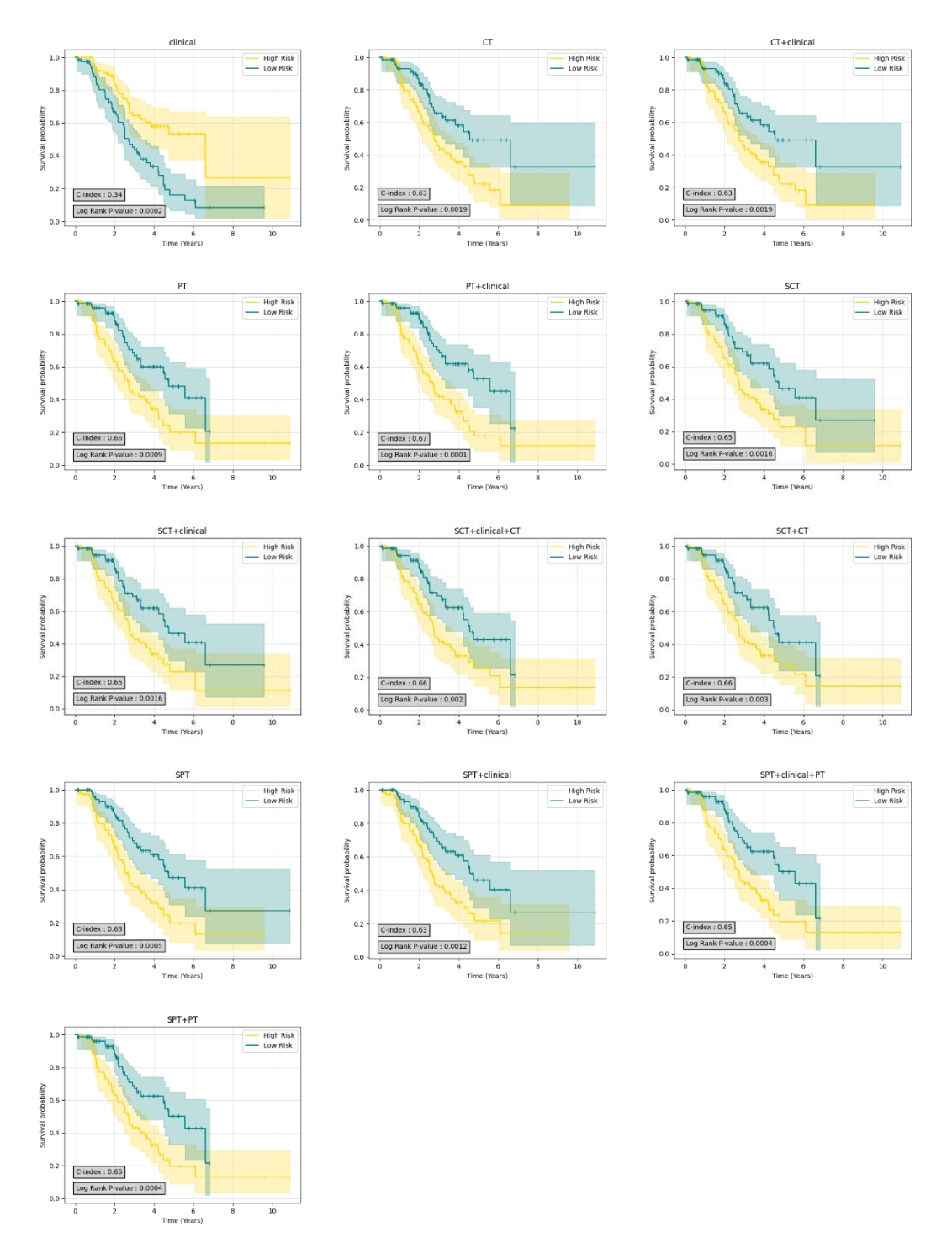
Supplemental Table S5. Hazard ratio survival analysis (HRSA) results

Dataset	PCA+ HRSA	FFCV c-index ±	FFCV p-	External Test	External Test
		STD	value	c-index	p-value
CF	CWGBSA	0.34±0.04	0	0.564	0.822
CT_HRF	CWGBSA	0.63 ± 0.08	0.002	0.656	0.019
CT_HRF+CF	CWGBSA	0.63 ± 0.08	0.002	0.653	0.118
PET_HRF	CWGBSA	0.66 ± 0.06	0.001	0.549	0.239
PET_HRF+CF	CWGBSA	0.67 ± 0.07	0	0.553	0.052
S_CT_DRF	CWGBSA	0.65 ± 0.07	0.002	0.547	0.021

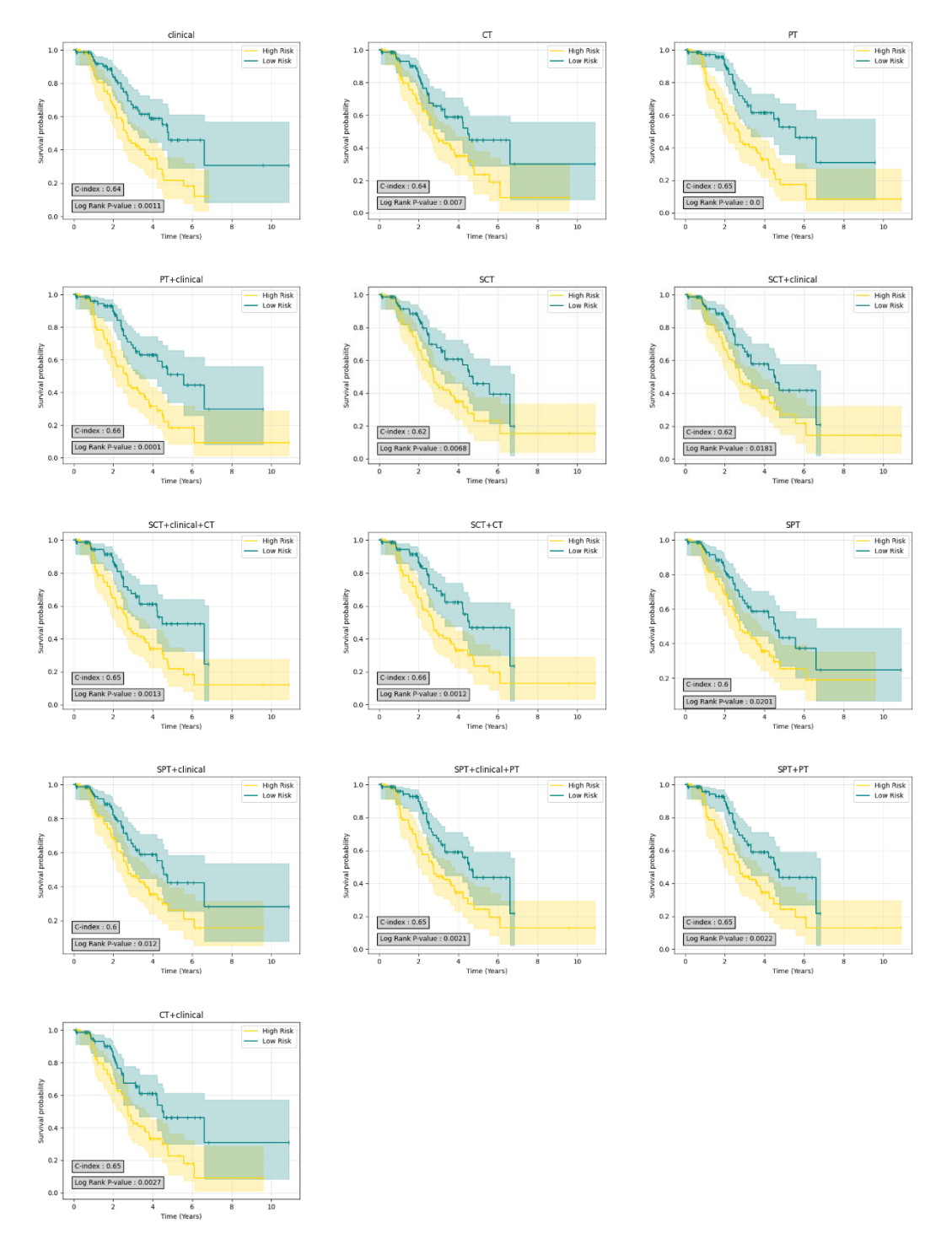
S_CT_DRF+CF	CWGBSA	0.65±0.06	0.002	0.551	0.085
$S_CT_DRF+CT_HRF$	CWGBSA	0.66 ± 0.06	0.003	0.598	0.632
$S_CT_DRF+CT_HRF+CF$	CWGBSA	0.66 ± 0.06	0.002	0.598	0.632
S_PET_DRF	CWGBSA	0.63 ± 0.06	0.001	0.46	0.611
S_PET_DRF+CF	CWGBSA	0.63 ± 0.06	0.001	0.471	0.452
$S_PET_DRF+PET_HRF$	CWGBSA	0.65 ± 0.06	0	0.538	0.921
$S_PET_DRF+PET_HRF+CF$	CWGBSA	0.65 ± 0.06	0	0.533	0.755
CF	FSSVM	0.64 ± 0.02	0.001	0.633	0.449
CT_HRF	FSSVM	0.64 ± 0.08	0.007	0.582	0.182
CT_HRF+CF	FSSVM	0.65 ± 0.08	0.003	0.598	0.141
PET_HRF	FSSVM	0.65 ± 0.07	0	0.56	0.209
PET_HRF+CF	FSSVM	0.66 ± 0.07	0	0.598	0.06
S_CT_DRF	FSSVM	0.62 ± 0.04	0.007	0.529	0.178
S_CT_DRF+CF	FSSVM	0.62 ± 0.04	0.018	0.527	0.178
$S_CT_DRF+CT_HRF$	FSSVM	0.66 ± 0.05	0.001	0.578	0.238
$S_CT_DRF+CT_HRF+CF$	FSSVM	0.65 ± 0.05	0.001	0.582	0.166
S_PET_DRF	FSSVM	0.60 ± 0.06	0.02	0.482	0.021
S_PET_DRF+CF	FSSVM	0.6 ± 0.05	0.012	0.48	0.01
$S_PET_DRF+PET_HRF$	FSSVM	0.65 ± 0.07	0.002	0.553	0.115

S_PET_DRF+PET_HRF+CF	FSSVM	0.65±0.06	0.002	0.553	0.115
CF	RSF	0.71 ± 0.05	0	0.613	0.263
CT_HRF	RSF	0.62 ± 0.05	0.052	0.521	0.742
CT_HRF+CF	RSF	0.64 ± 0.12	0.001	0.523	0.886
PET_HRF	RSF	0.65 ± 0.06	0.002	0.573	0.628
PET_HRF+CF	RSF	0.65 ± 0.06	0	0.569	0.107
S_CT_DRF	RSF	0.61 ± 0.05	0.014	0.553	0.075
S_CT_DRF+CF	RSF	0.61 ± 0.02	0.025	0.556	0.027
$S_CT_DRF+CT_HRF$	RSF	0.66 ± 0.05	0	0.632	0.585
$S_CT_DRF+CT_HRF+CF$	RSF	0.62 ± 0.05	0.004	0.598	0.335
S_PET_DRF	RSF	0.59 ± 0.03	0.229	0.509	0.068
S_PET_DRF+CF	RSF	0.58 ± 0.05	0.021	0.513	0.371
$S_PET_DRF+PET_HRF$	RSF	0.63 ± 0.06	0.02	0.587	0.207
S_PET_DRF+PET_HRF+CF	RSF	0.62±0.09	0.173	0.56	0.004

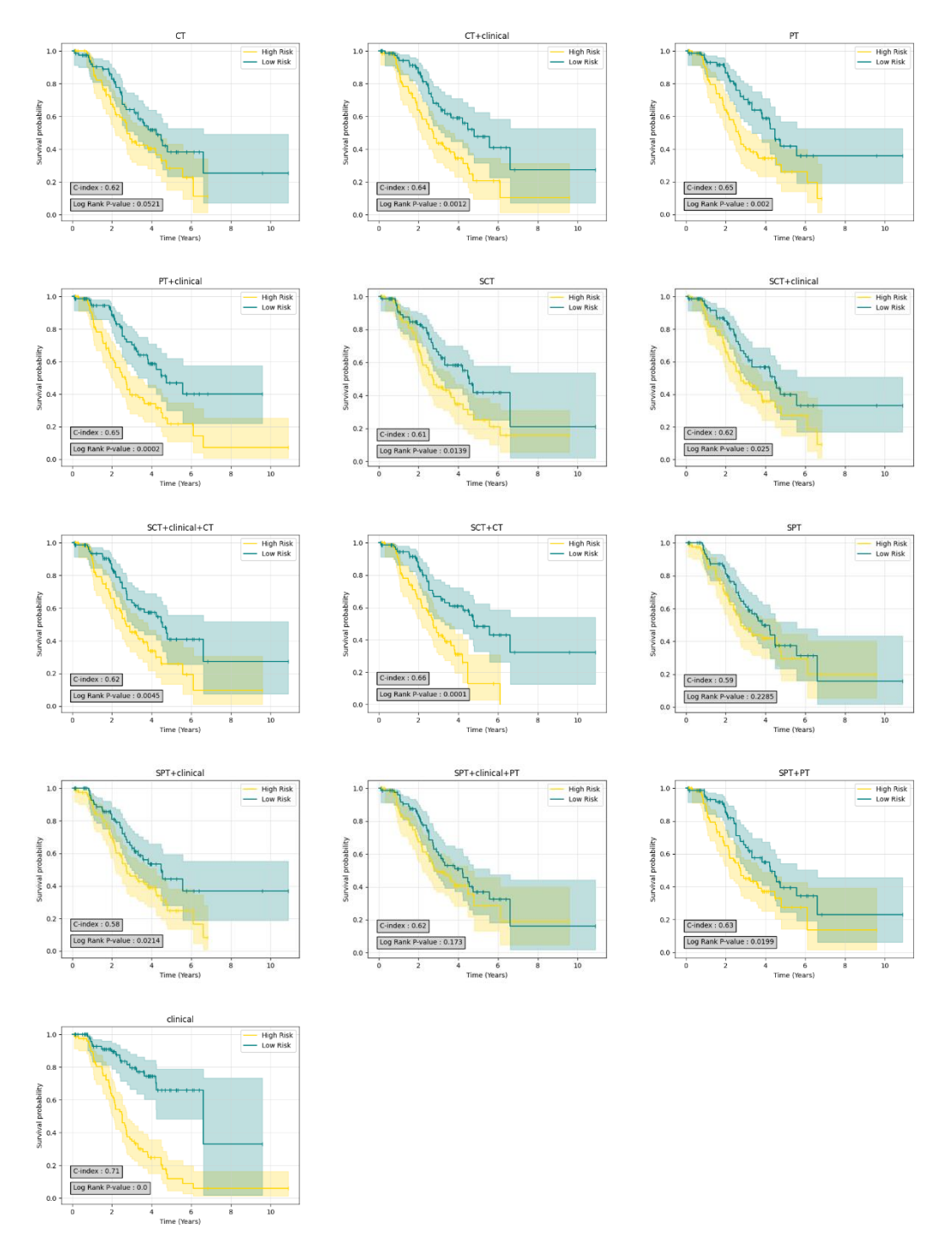
HRF: handcrafted Radiomics features, DRF: deep Radiomics features, DRF_CT: DRFs extracted from segmented CT, DRF_PET: DRFs extracted from segmented PET, HRF_CT: HFRs extracted from segmented CT, HRF_PET: HFRs extracted from segmented PET, FSSVM: Fast Survival Support Vector Machines, CWGBSA: Component-wise Gradient Boosting Survival Analysis, RSF: Random Survival Forest, FFCV: Five-Fold Cross-Validation, HRSA: Hazard Ratio Survival Analysis. PCA: Principal Component Analysis.



Supplemental Figure S2. Kaplan-Meier survival curves generated for Component-wise Gradient Boosting Survival Analysis (CWGBSA) Results; SCT: Deep Radiomics Features extracted from CT, CT: Handcrafted Radiomics Features Extracted From CT, SPET: Deep Radiomics Features extracted from PET, PET: Handcrafted Radiomics Features Extracted From PET



Supplemental Figure S3. Kaplan-Meier survival curves generated for Fast Survival Support Vector Machines (FSSVM) Results; SCT: Deep Radiomics Features extracted from CT, CT: Handcrafted Radiomics Features Extracted From CT, SPET: Deep Radiomics Features extracted from PET, PET: Handcrafted Radiomics Features Extracted From PET



Supplemental Figure S4. Kaplan-Meier survival curves generated for Random Survival Forest (RSF) Results; SCT: Deep Radiomics Features extracted from CT, CT: Handcrafted Radiomics Features Extracted From CT, SPET: Deep Radiomics Features extracted from PET, PET: Handcrafted Radiomics Features Extracted From PET

References

- [1] D. I. Garcia and C. Catana, "MR Imaging-Guided Attenuation Correction of PET Data in PET/MR Imaging," *PET Clin*, vol. 11, no. 2, pp. 129-49, 2016.
- [2] M. C. Adams, T. G. Turkington, J. M. Wilson and T. Z. Wong, "A systematic review of the factors affecting accuracy of SUV measurements.," *American Journal of Roentgenology.*, vol. 195, no. 2, pp. 310-320, 2010.
- [3] J. Han, M. Kamber and J. Pei, Data Mining: Concepts and Techniques, San Francisco, CA, USA: Elsevier, 2011.
- [4] A. Jain, R. P. W. Duin and J. Mao, "Statistical pattern recognition: a review," *IEEE Transactions on Pattern Analysis and Machine Intelligence*, vol. 22, no. 1, pp. 4-37, 2000.
- [5] M. R. Salmanpour, I. Shiri and et al, "ViSERA: Visualized & Standardized Environment for Radiomics Analysis - A Shareable, Executable, and Reproducible Workflow Generator," in 2023 IEEE Nuclear Science Symposium, Medical Imaging Conference and International Symposium on Room-Temperature Semiconductor Detectors (NSS MIC RTSD), Vancouver, 2023.
- [6] The scikit-learn developers, "sklearn.feature_selection.r_regression," scikit-learn, 2025. [Online]. Available: https://scikit-learn.org/stable/modules/generated/sklearn.feature_selection.r_regression.html. [Accessed 22 August 2024].
- [7] The scikit-learn developers, "sklearn.feature_selection.f_regression," scikit-learn, 2025. [Online]. Available: https://scikit-learn.org/stable/modules/generated/sklearn.feature_selection.f_regression.html. [Accessed 22 August 2024].
- [8] M. Salmanpour, M. Bakhtiyari and et al, "Application of novel hybrid machine learning systems and radiomics features for non-motor outcome prediction in Parkinson's disease," *Physics in Medicine & Biology*, vol. 68, no. 3, p. 035004, 2023.
- [9] M. J. Crowther, P. Royston and M. Clements, "A flexible parametric accelerated failure time model and the extension to time-dependent acceleration factors," *Biostatistics*, vol. 24, no. 3, pp. 811-831, 2023.

- [10] N. Ghorbani, J. Yazdani-Charati and et al, "Application of the Weibull Accelerated Failure Time Model in the Determination of Disease-Free Survival Rate of Patients with Breast Cancer," *Iranian Journal Of Health Sciences*, vol. 4, no. 2, pp. 11-18, 2016.
- [11] R. K. Halder, M. N. Uddin and et al, "Enhancing K-nearest neighbor algorithm: a comprehensive review and performance analysis of modifications," *Journal of Big Data*, vol. 11, no. 1, p. 113, 2024.
- [12] Y. Freund and R. E. Schapire, "A decision-theoretic generalization of on-line learning and an application to boosting," *Journal of Computer and System Sciences*, vol. 55, no. 1, p. 119–139, 1997.
- [13] T. K. Ho, "Random Decision Forests," in *Proceedings of the 3rd International Conference on Document Analysis and Recognition*, Montreal, QC, August 1995.
- [14] G. Cybenko, "Approximation by superpositions of a sigmoidal function," *Math. Control Signal Systems*, vol. 303–314, 1989.
- [15] A. M. Ahmed, A. Rizaner and A. H. Ulusoy, "A Decision Tree Algorithm Combined with Linear Regression," in *International Conference on Computer, Control, Electrical, and Electronics Engineering (ICCCEEE)*, Khartoum, Sudan, 2018.
- [16] X. Yan, "Linear Regression Analysis: Theory and Computing," *World Scientific*, Vols. pp. 1–2, ISBN 9789812834119, 2009.
- [17] C. Cortes and V. Vapnik, "Support-vector networks," *Machine Learning.*, vol. 20 (3);273–297, 1995.
- [18] S. Pölsterl, "A Library for Time-to-Event Analysis Built on Top of scikit-learn," *Journal of Machine Learning Research*, vol. 21, no. 212, p. 1–6, 2020.
- [19] S. Pölsterl, "Gradient Boosted Models," 2020. [Online]. Available: https://scikit-survival.readthedocs.io/en/stable/user_guide/boosting.html. [Accessed 9 January 2024].
- [20] S. Pölsterl, "Random survival forests," 2020. [Online]. Available: https://scikit-survival.readthedocs.io/en/stable/user_guide/random-survival-forest.html. [Accessed 9 January 2024].

[21] P. Cascante-Bonilla, F. Tan and et al, "Curriculum Labeling: Revisiting Pseudo-Labeling for Semi-Supervised Learning," *Proceedings of the AAAI Conference on Artificial Intelligence*, vol. 35, no. 8, pp. 6912-6920, 2021.